



Scanning Tunneling Microscopy in Surface Science, Nanoscience and Catalysis

*Edited by
Michael Bowker and Philip R. Davies*



**WILEY-
VCH**

WILEY-VCH Verlag GmbH & Co. KGaA

**Scanning Tunneling Microscopy
in Surface Science, Nanoscience
and Catalysis**

*Edited by
Michael Bowker and Philip R. Davies*

Further Reading

K.W. Kolasinski

Surface Science

**Foundations of Catalysis
and Nanoscience**

2008

ISBN: 978-0-470-03304-3

D.G. Brandon, W.D. Kaplan

Microstructural Characterization of Materials

2008

ISBN: 978-0-470-02784-4

J.W. Niemantsverdriet

Spectroscopy in Catalysis An Introduction

2007

ISBN: 978-3-527-31651-9

B.P. Jena, J.K.H. Hoerber (Eds.)

Force Microscopy

Applications in Biology and Medicine

2006

ISBN: 978-0-471-39628-4

M. Prutton, M. El Gomati (Eds.)

Scanning Auger Electron Microscopy

2006

ISBN: 978-0-470-86677-1

D.K. Schroder

Semiconductor Material and Device Characterization

2006

ISBN: 978-0-471-73906-7

Scanning Tunneling Microscopy in Surface Science, Nanoscience and Catalysis

Edited by
Michael Bowker and Philip R. Davies



WILEY-VCH Verlag GmbH & Co. KGaA

The Editors

Prof. Michael Bowker

Cardiff University
Wolfson Nanoscience Lab and
Cardiff Catalysis Institute
School of Chemistry
Cardiff, CF10 3AT
United Kingdom

Dr. Philip R. Davies

Cardiff University
Wolfson Nanoscience Lab and
Cardiff Catalysis Institute
School of Chemistry
Cardiff, CF10 3AT
United Kingdom

Cover illustration

The STM images being past of the front cover picture have been kindly provided by the group of D. Wayne Goodman (authors of Chapter 3).

All books published by Wiley-VCH are carefully produced. Nevertheless, authors, editors, and publisher do not warrant the information contained in these books, including this book, to be free of errors. Readers are advised to keep in mind that statements, data, illustrations, procedural details or other items may inadvertently be inaccurate.

Library of Congress Card No.: applied for

British Library Cataloguing-in-Publication Data

A catalogue record for this book is available from the British Library.

**Bibliographic information published by
the Deutsche Nationalbibliothek**

The Deutsche Nationalbibliothek lists this publication in the Deutsche Nationalbibliografie; detailed bibliographic data are available on the Internet at <http://dnb.d-nb.de>

© 2010 WILEY-VCH Verlag GmbH & Co. KGaA, Weinheim

All rights reserved (including those of translation into other languages). No part of this book may be reproduced in any form – by photoprinting, microfilm, or any other means – nor transmitted or translated into a machine language without written permission from the publishers. Registered names, trademarks, etc. used in this book, even when not specifically marked as such, are not to be considered unprotected by law.

Printed in the Federal Republic of Germany
Printed on acid-free paper

Cover Design Formgeber, Eppelheim

Typesetting Thomson Digital, Noida, India

Printing Strauss GmbH, Mörlenbach

Bookbinding Litges & Dopf Buchbinderei GmbH, Heppenheim

ISBN: 978-3-527-31982-4

Contents

Preface IX

List of Contributors XIII

1	Chirality at Metal Surfaces	1
	<i>Chris J. Baddeley and Neville V. Richardson</i>	
1.1	Introduction	1
1.1.1	Definition of Chirality	1
1.1.2	Nomenclature of Chirality: The (R),(S) Convention	2
1.2	Surface Chirality Following Molecular Adsorption	4
1.2.1	Achiral Molecules on Achiral Surfaces	4
1.2.2	Lattice Matching	8
1.2.3	Chiral Molecules on Achiral Surfaces	12
1.2.4	Chiral Molecules on Chiral Surfaces	15
1.2.5	Chiral Etching	16
1.3	Chiral Amplification and Recognition	19
1.3.1	Chiral Amplification in Two Dimensions	19
1.3.2	Chiral Switching	20
1.3.3	Chiral Recognition	21
1.3.4	Prochiral Molecules Interacting with Chiral Surfaces	24
1.4	Conclusions	25
	References	26
2	The Template Route to Nanostructured Model Catalysts	29
	<i>Conrad Becker and Klaus Wandelt</i>	
2.1	Introduction	29
2.2	Surfaces as Two-Dimensional Templates	31
2.3	STM Imaging of Oxide Films	34
2.4	STM Imaging of Metal Particles on Oxide Films	39
2.5	Template-Controlled Growth of Model Catalysts	44
2.5.1	Oxides as Templates	44

2.5.2	Modified Templates	50
2.6	Conclusions	51
	References	52
3	<i>In Situ</i> STM Studies of Model Catalysts	55
	<i>Fan Yang and D. Wayne Goodman</i>	
3.1	Introduction	55
3.2	Instrumentation	56
3.3	Visualizing the Pathway of Catalytic Reactions	59
3.3.1	Imaging of Adsorbates and Reaction Intermediates	59
3.3.2	Imaging Chemisorption on Metals	61
3.3.3	Determining the Sites for Chemisorption on Oxide Surfaces	64
3.3.4	Visualizing Reaction Intermediates and the Mechanism of Hydrogen Oxidation	71
3.3.5	Measuring the Reaction Kinetics of CO Oxidation	73
3.4	Metal Surfaces at High Pressures	81
3.5	<i>In Situ</i> Studies of Supported Model Catalysts	85
3.5.1	Monitoring the Growth Kinetics of Supported Metal Catalysts	85
3.5.2	Studies of the SMSI Effect	88
3.5.3	Sintering Kinetics of Supported Au Clusters	89
3.6	Outlook	91
	References	92
4	Theory of Scanning Tunneling Microscopy and Applications in Catalysis	97
	<i>Gilberto Teobaldi, Haiping Lin, and Werner Hofer</i>	
4.1	Catalysis and Scanning Tunneling Microscopy	97
4.2	Image Formation in an STM	98
4.3	Simulating Tunneling Currents	99
4.4	Simulating Chemical Reactivity	100
4.5	Catalytic Water Production	101
4.5.1	TiO ₂ : A Catalytic Model System	106
4.6	Outlook	115
	References	116
5	Characterization and Modification of Electrode Surfaces by <i>In Situ</i> STM	119
	<i>Dieter M. Kolb and Felice C. Simeone</i>	
5.1	Introduction	119
5.2	<i>In Situ</i> STM: Principle, Technical Realization and Limitations	120
5.2.1	Principle Considerations for <i>In Situ</i> Operation	120
5.2.2	Technical Realization	124
5.2.2.1	Tip Preparation and Isolation	124
5.2.2.2	Electrochemical Cell	126
5.2.2.3	Vibration Damping	127

5.2.3	Limitations	127
5.3	Imaging Single-Crystal Surfaces of Catalytically Relevant Systems	128
5.3.1	Preparation and Imaging of Metal Single-Crystal Surfaces	128
5.3.2	Bimetallic Surfaces	130
5.4	Strategies for Nanostructuring Surfaces	132
5.4.1	Oxidation–Reduction Cycles for Roughening and Faceting Surfaces	132
5.4.2	Surface Modification by an STM: An Overview	134
5.4.3	Metal Nanocluster Deposition via Jump-to-Contact	139
	References	144
6	STM Imaging of Oxide Nanolayer Model Systems	147
	<i>Falko P. Netzer and Svetlozar Surnev</i>	
6.1	Introduction	147
6.2	Experimental Aspects and Technical Developments	149
6.3	Case Studies: Selected Oxide–Metal Systems	152
6.3.1	Alumina Nanolayers on NiAl Alloys	152
6.3.2	Titanium Oxide Nanolayers	155
6.3.3	Vanadium Oxide Nanolayers	159
6.3.4	Iron Oxides on Pt(1 1 1)	169
6.3.5	Nickel Oxide Nanolayers	173
6.3.6	Ceria Nanolayers on Metal Surfaces	177
6.4	Synopsis and Outlook	182
	References	183
7	Surface Mobility of Atoms and Molecules Studied with High-Pressure Scanning Tunneling Microscopy	189
	<i>Gabor A. Somorjai, Feng Tao, and Derek Butcher</i>	
7.1	Introduction	189
7.2	Characterization of Surface Mobility of Molecules and Atoms	189
7.3	High-Pressure STM Technique and Instrumentation	191
7.4	Mobility and Flexibility of Catalyst Surfaces at High-Pressure High-Temperature Reaction Conditions	197
7.5	Adsorbate Mobility During Catalytic Reactions	206
7.5.1	Ethylene Hydrogenation on Pt(1 1 1)	207
7.5.2	Hydrogenation of C ₆ Cyclic Hydrocarbons on Pt(1 1 1)	209
7.5.3	CO/NO Coadsorption on Rh(1 1 1)	213
7.6	Summary	216
	References	216

8 Point Defects on Rutile $\text{TiO}_2(1\ 1\ 0)$: Reactivity, Dynamics, and Tunability 219*Chi L. Pang and Geoff Thornton*

8.1 Introduction 219

8.2 Methods 220

8.3 Water Dissociation at Oxygen Vacancies and the Identification of Point Defects 221

8.4 O_2 Dissociation at Oxygen Vacancies 229

8.5 Alcohol Dissociation at Oxygen Vacancies 229

8.6 Diffusion of Oxygen Vacancies and Surface Hydroxy 232

8.7 Tuning the Densities of Oxygen Vacancies and Surface Hydroxyl on $\text{TiO}_2(1\ 1\ 0)$ 234

8.8 Outlook 236

References 236

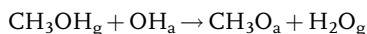
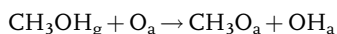
Index 239

Preface

The objective of this book is to highlight the important strides being made toward a molecular understanding of the processes that occur at surfaces through the unique information provided by the proximal scanning probe family of techniques: this principally involves scanning tunneling microscopy (STM) but some atomic force microscopy (AFM) experiments are also included.

The chapters in this book describe several *state-of-the-art* examples where an atomic understanding of surface processes is developing out of atomically resolved information provided by STM and AFM. The focus of much of the work is on understanding the fundamentals of catalysis, a reflection of the huge significance of heterogeneous catalysis in society today, but the discoveries being made in this field will undoubtedly have a much wider significance in the field of nanoscience/technology.

Reaction equations are derived from the results of global reaction measurements and considerations of stoichiometry. Until recently, the intermediates (and in particular the surface species) involved in the mechanism and their spatial location have remained largely theoretical. The advent of STM has, for the first time, allowed us the possibility of getting direct insight into this area. An example is the molecular identification of the sequence of reaction steps and of the species involved in the reaction of gas-phase methanol with oxygen on a copper surface. This produces methoxy groups as the first step, in which the slightly acidic hydrogen from the alcohol is stripped by surface oxygen leading to water desorption, as shown below, where the subscript “a” refers to an adsorbed species.



In this case, as in many others, STM has enabled us to identify the active sites at which reaction between methanol and adsorbed oxygen takes place, and has also allowed us to verify, at the atomic and the molecular scale, that the reaction does indeed occur in the way the above stoichiometric equations describe. This is invaluable information in the quest to understand and improve catalytic processes.

The principal advantage of the probe methods is their extraordinary spatial resolution (<0.1 nm) that does not, by necessity, require large areas of order. Their potential is further expanded by the ability to study surfaces under conditions that range from ultrahigh vacuum at cryogenic temperatures to industrially relevant pressures and temperatures to aggressive liquid phases. A major aim is to identify surface structures and intermediates present during operation *in situ* and *in operando*. There are three principal requirements to achieve these objectives: (i) high-pressure operation (already demonstrated by a number of individual groups in the field); (ii) the ability to image at high temperature while at high pressure (to some degree, this has been achieved, although there are limitations to the temperature range that can be studied, especially at above ambient pressure); (iii) fast scanning (of the order of 1–10 images per second) since catalytic turnover rates are often very high (e.g., 10 s^{-1}). This is also important for the ultimate aim of determining the statistics of the reaction (e.g., determining directly, *in situ*, the turnover number for the reaction). The authors believe that these aims will be realized in the next 10 years or so, but we are not quite there yet. There is plenty of room in the field for further developments.

It is fitting that this book should include a contribution from the laboratory of Somorjai, one of the principal exponents of the surface science approach to catalysis, who has developed a number of new approaches to the field and who, in recent years, has looked, in particular, at adsorption and surface reactions at high gas pressures. He reviews this work with some considerable and helpful focus on equipment developments. Similarly, Goodman has been a strong advocate of *in situ* high-pressure studies and has been at the forefront of developments in the field for some considerable time. He reviews the state of the art and generously acknowledges the contribution of colleagues in the field, some of whom have contributed to this volume.

Kolb and Simeone discuss the application of STM to samples in the liquid environment and deposition of metal from the STM tip itself, via reaction and neutralization of cations from solution, generating reproducible patterns at nanometer scales. The ability to control nanoparticle formation in terms of constant spacing, spatial arrangement, and monosized dispersion is a crucial one for future nanotechnology developments and Becker and Wandelt have also concerned themselves with the synthesis of reproducible patterns of particles at the nanoscale. They illustrate the potential of a bottom-up process, by gas-phase metal deposition, for generating model catalysts that can be studied both by spatially averaging techniques and by scanning tunneling microscopy.

Netzer and Surnev consider the problem of generating model catalyst systems for study using STM from a different direction. They examine the growth of thin oxide films on metal substrates, the “inverse” catalyst approach, and show the intrinsic beauty in the geometrical arrangements of thin-layer oxides that can be obtained when high-quality imaging is pursued. They also report the formation of new types of oxide structure in the 2D regime. Importantly, they give consideration to the particular problems of interpretation posed by STM images of thin oxide layers. Since STM images involve a convolution of the substrate, adsorbate, and STM tip

electronic states, interpretation of STM images is critical to all of the work presented in this book and the contribution by Hofer, Lin, and Teobaldi is particularly welcome since it provides a detailed review of the advances made in the theory of STM imaging, highlighting areas where theory now has a good grasp of the issues and where further development is needed.

The ability of STM to image at the atomic scale is particularly exemplified by the two other chapters in the book. Thornton and Pang discuss the identification of point defects at TiO_2 surfaces, a material that has played an important role in model catalyst studies to date. Point defects have been suggested to be responsible for much of the activity at oxide surfaces and the ability to identify these features and track their reactions with such species as oxygen and water represents a major advance in our ability to explore surface reactions. Meanwhile, Baddeley and Richardson concentrate on the effects of chirality at surfaces, and on the important field of surface chirality and its effects on adsorption, in a chapter that touches on one of the fundamental questions in the whole of science – the origins of life itself!

In recent years, studies using STM have expanded from the use of the atomically flat metal single crystals that have been the mainstay of surface science since the mid-1960s to complex oxide surfaces and to 3D nanoparticles, often grown on representative catalyst supports. The improvement in the technology and interpretation of imaging, and the increasing complexity of the surfaces being studied, ensures a pivotal role in the future for surface science, particularly in the context of the increasing practical importance of nanoscience in technological development.

Cardiff University,
December 2009

Michael Bowker and Philip R. Davies

List of Contributors

Chris J. Baddeley

University of St Andrews
EaStCHEM School of Chemistry
St Andrews
Fife, KY16 9ST
UK

Conrad Becker

Université de la Méditerranée
CINaM – CNRS – UPR3118
Campus de Luminy
Case 913
13288 Marseille Cedex 9
France

Derek Butcher

Lawrence Berkeley National
Laboratory
Materials Science and Chemistry
Divisions
Berkeley, CA 94720
USA
and
University of California
Department of Chemistry
Berkeley, CA 94720
USA

D. Wayne Goodman

Texas A&M University
Department of Chemistry
P.O. Box 30012
College Station, TX 77843-3012
USA

Werner Hofer

The University of Liverpool
Surface Science Research Centre
Liverpool, L69 3BX
UK

Dieter M. Kolb

University of Ulm
Institute of Electrochemistry
89069 Ulm
Germany

Haiping Lin

The University of Liverpool
Surface Science Research Centre
Liverpool, L69 3BX
UK

Falko P. Netzer

Karl Franzens University Graz
Institute of Physics, Surface and
Interface Physics
8010 Graz
Austria

Chi L. Pang

University College London
London Centre for Nanotechnology
and Department of Chemistry
London, WC1H 0AJ
UK

Neville V. Richardson

University of St Andrews
EaStCHEM School of Chemistry
St Andrews
Fife, KY16 9ST
UK

Felice C. Simeone

University of Ulm
Institute of Electrochemistry
89069 Ulm
Germany

Gabor A. Somorjai

Lawrence Berkeley National
Laboratory
Materials Science and Chemistry
Divisions
Berkeley, CA 94720
USA
and
University of California
Department of Chemistry
Berkeley, CA 94720
USA

Svetlozar Surnev

Karl Franzens University Graz
Institute of Physics, Surface and
Interface Physics
8010 Graz
Austria

Feng Tao

Lawrence Berkeley National
Laboratory
Materials Science and Chemistry
Divisions
Berkeley, CA 94720
USA
and
University of California
Department of Chemistry
Berkeley, CA 94720
USA

Gilberto Teobaldi

The University of Liverpool
Surface Science Research Centre
Liverpool, L69 3BX
UK

Geoff Thornton

University College London
London Centre for Nanotechnology
and Department of Chemistry
London, WC1H 0AJ
UK

Klaus Wandelt

Universität Bonn
Institut für Physikalische und
Theoretische Chemie
Wegelerstrasse 12
53115 Bonn
Germany

Fan Yang

Texas A&M University
Department of Chemistry
P.O. Box 30012
College Station, TX 77843-3012
USA

1

Chirality at Metal Surfaces

Chris J. Baddeley and Neville V. Richardson

1.1

Introduction

Since the mid-1990s, the number of surface science investigations of chirality at surfaces has increased exponentially. Advances in the technique of scanning tunneling microscopy (STM) have been crucial in enabling the visualization of single chiral molecules, clusters, and extended arrays. As such, STM has facilitated dramatic advances in the fundamental understanding of the interactions of chiral molecules with surfaces and the phenomena of chiral amplification and chiral recognition. These issues are of considerable technological importance, for example, in the development of heterogeneous catalysts for the production of chiral pharmaceuticals and in the design of biosensors. In addition, the understanding of chirality at surfaces may be a key to unraveling the complexities of the origin of life.

1.1.1

Definition of Chirality

The word chirality is derived from the Greek *kheir* meaning “hand.” It is the geometric property of an object that distinguishes a right hand from a left hand. Lord Kelvin provided a definition of chirality in his 1884 Baltimore Lectures, “I call any geometrical figure or group of points ‘chiral’ and say it has ‘chirality’, if its image in a plane mirror, ideally realized, cannot be brought into coincidence with itself.” For an isolated object, for example, a molecule, the above statement can be interpreted as being equivalent to requiring that the object possesses neither a mirror plane of symmetry nor a point of symmetry (center of inversion). If a molecule possesses either one of these symmetry elements, it can be superimposed on its mirror image and is therefore *achiral*. A chiral molecule and its mirror image are referred to as being a pair of *enantiomers*. Many organic molecules possess the property of chirality. Chiral centers are most commonly associated with the tetrahedral coordination of four different substituents. However, there are many examples of other rigid

structures that have chiral properties where a significant barrier exists to conformational change within the molecule.

1.1.2

Nomenclature of Chirality: The *(R)*,*(S)* Convention

Most of the physical properties (e.g., boiling and melting point, density, refractive index, etc.) of two enantiomers are identical. Importantly, however, the two enantiomers interact differently with polarized light. When plane polarized light interacts with a sample of chiral molecules, there is a measurable net rotation of the plane of polarization. Such molecules are said to be optically active. If the chiral compound causes the plane of polarization to rotate in a clockwise (positive) direction as viewed by an observer facing the beam, the compound is said to be dextrorotatory. An anticlockwise (negative) rotation is caused by a levorotatory compound. Dextrorotatory chiral compounds are often given the label *D* or (+) while levorotatory compounds are denoted by *L* or (–).

In this chapter, we will use an alternative convention that labels chiral molecules according to their absolute stereochemistry. The *(R)*,*(S)* convention or Cahn–Ingold–Prelog system was first introduced by Robert S. Cahn and Sir Christopher K. Ingold (University College, London) in 1951 and later modified by Vlado Prelog (Swiss Federal Institute of Technology) [1]. Essentially, the four atomic substituents at a stereocenter are identified and assigned a priority (1 (highest), 2, 3, 4 (lowest)) by atomic mass. If two atomic substituents are the same, their priority is defined by working outward along the chain of atoms until a point of difference is reached. Using the same considerations of atomic mass, the priority is then assigned at the first point of difference. For example, a $-\text{CH}_2-\text{CH}_3$ substituent has a higher priority than a $-\text{CH}_3$ substituent. Once the priority has been assigned around the stereocenter, the tetrahedral arrangement is viewed along the bond between the central atom and the lowest priority (4) substituent (often a C–H bond) from the opposite side to the substituent (Figure 1.1). If the three other substituents are arranged such that the path from 1 to 2 to 3 involves a clockwise rotation, the stereocenter is labeled *(R)* (Latin *rectus* for right). By contrast, if the path involves an anticlockwise rotation, the stereocenter is labeled *(S)* (Latin *sinister* for left). It is important to note that the absolute stereochemistry cannot be predicted from the *L* or *D* labels and vice versa.

In nature, a remarkable, and so far unexplained, fact is that the amino acid building blocks of all proteins are exclusively left-handed and that the sugars contained within the double helix structure of DNA are exclusively right-handed. The consequences of the chirality of living organisms are far reaching. The human sense of smell, for example, is able to distinguish between pure *(R)*-limonene (smelling of oranges) and *(S)*-limonene (smelling of lemons). More significantly, two enantiomeric forms of an organic molecule can have different physiological effects on human body. In many cases, one enantiomer is the active component while the opposite enantiomer has no effect (e.g., ibuprofen where the *(S)*-enantiomer is active). However, often the two enantiomers have dramatically different effects. For example, *(S)*-methamphetamine

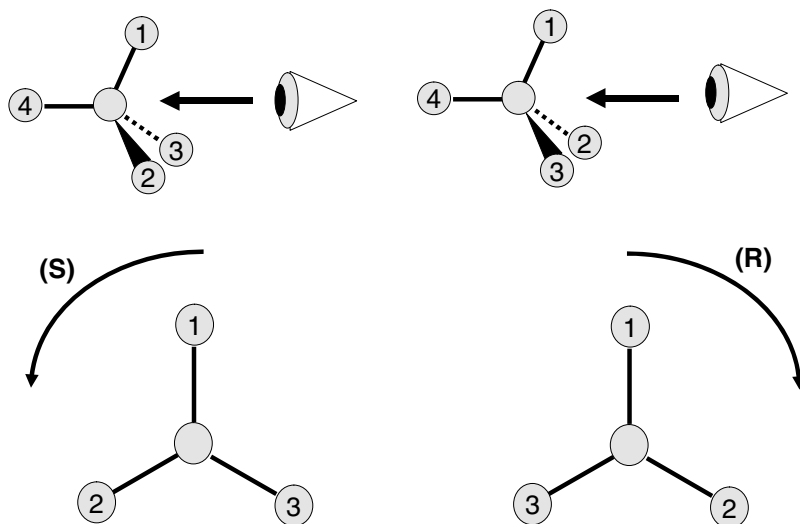


Figure 1.1 Schematic diagram explaining the Cahn–Ingold–Prelog convention for determining the absolute stereochemistry of a chiral molecule.

is a psychostimulant while (*R*)-methamphetamine is the active ingredient in many nasal decongestants (Figure 1.2).

In the pharmaceutical industry, about half of all of the new drugs being tested require the production of exclusively one enantiomeric product. Thermodynamically, this is a challenging problem since the two isolated enantiomers have identical Gibbs energies; the reaction from prochiral reagent to product should therefore result in a 50 : 50 (*racemic*) mixture at equilibrium. To skew the reaction pathway to form one product with close to 100% enantioselectivity is nontrivial. Knowles [2], Noyori [3], and Sharpless [4] were awarded the Nobel Prize in Chemistry in 2001 for developing enantioselective homogeneous catalysts capable of producing chiral molecules on an industrial scale. Typically, these catalysts consist of organometallic complexes with chiral ligands. Access to the metal center by the reagent is strongly sterically influenced by the chiral ligands resulting in preferential formation of one enantiomeric product. There are many potential advantages of using heterogeneous catalysts, not least the ease of separation of the catalyst from the products. However, despite extensive research over several decades, relatively few successful catalysts have been synthesized on a laboratory scale and the impact on industrial catalysis is essentially negligible. One of the primary motivations behind surface science studies of chirality at surfaces is to understand the surface chemistry underpinning chiral catalysis and to develop methodologies for the rational design of chiral catalysts. Similarly, those interested in issues related to the origin of life are investigating the possibility that surfaces were responsible for the initial seeding of the chiral building blocks of life and that, presumably via some chiral amplification effects, this led to the overwhelming dominance of left-handed amino acids and right-handed sugars in

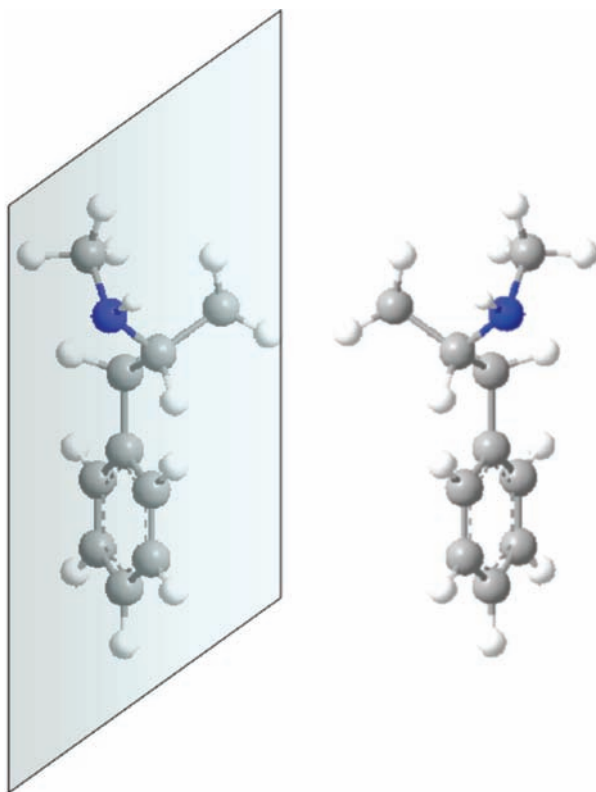


Figure 1.2 The two mirror equivalent forms of the drug methamphetamine. On the right is shown the (*S*)-form of the molecule; on the left is the (*R*)-enantiomer.

biological systems on Earth. As such, the surface chemistry of chiral solids, chiral amplification, and chiral recognition are all important subtopics of chiral surface science. STM has proved to be the single most important tool of researchers in this field.

1.2

Surface Chirality Following Molecular Adsorption

1.2.1

Achiral Molecules on Achiral Surfaces

When a molecule is adsorbed on a surface, the symmetry of the combined adsorbate–substrate system is very likely to be reduced compared to that of the isolated gas-phase species or the bare adsorption site. This raises the possibility that, if mirror planes present in the isolated achiral molecule and those at the relevant

adsorption site of the clean surface are not coincident, then the combined system of a single adsorbed molecule and the substrate will be locally chiral; that is, mirror planes of the isolated molecule are lost on adsorption and chirality is *induced* by the adsorption process. Note that a center of symmetry, also capable of ensuring superimposability of an object and its mirror image, is necessarily incompatible with the presence of a nearby surface [5]. A commonly observed case of such adsorption-induced chirality is that of a planar molecule with C_s symmetry (a single mirror plane) in the gas phase adsorbing on a surface such that the molecular plane is parallel to the substrate, as favored, for example, by van der Waals (vdW) interactions, thereby destroying the mirror plane symmetry. The molecule can then exist in two enantiomeric forms, although necessarily as a racemic mixture in the absence of any other influences that might lead to a preference of one rather than the other. Figure 1.3 illustrates this possibility for 4-[*trans*-2-(pyrid-4-yl-vinyl)]benzoic acid (PVBA) adsorbed parallel to an idealized, unstructured surface [6]

Interconversion of the two enantiomers is possible only if the molecule is removed from the surface and rotated by 180° around an axis parallel to the substrate surface. In the case of PVBA adsorbed on $\text{Ag}\{1\ 1\ 1\}$, hydrogen bonding leads to a preference for homochiral double chains based on head-to-tail $\text{N}-\text{H}\cdots\text{O}$ bonds and a C_2 axis relating the two strands of the chains. The chirality of the chain can be recognized in the STM images by the stagger of one strand relative to the other that arises from $\text{C}-\text{H}\cdots\text{O}$ bonds, as shown in Figure 1.3 [6].

The example described above is that of the separation of enantiomers into 1D chains following adsorption-induced chirality. In addition to forming chirally seg-

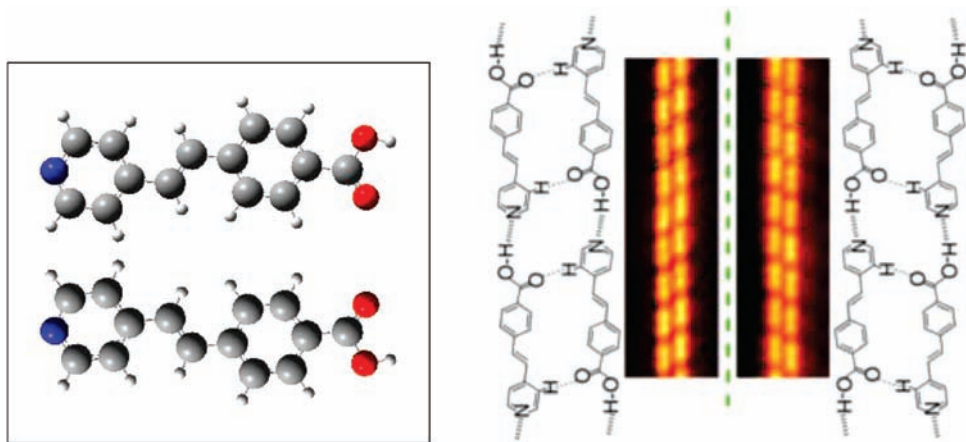


Figure 1.3 Molecular models showing the two enantiomers resulting from the loss of mirror plane symmetry on adsorption with the molecular plane parallel to the substrate. The separation of enantiomers observed by STM is identified by the relative displacement of adjacent monomers within the double chain. (Reprinted with permission from Ref. [6]. Copyright 2001, American Physical Society.)

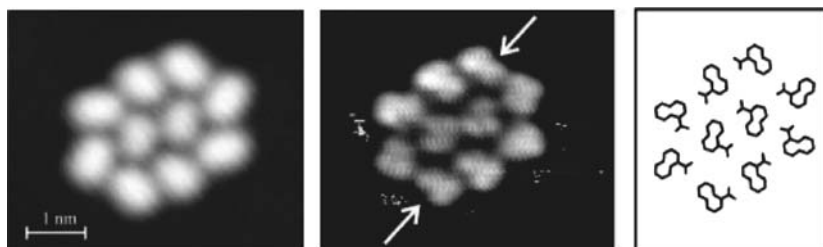


Figure 1.4 Low- and high-resolution STM images of a decamer of 1-nitronaphthalene, together with the minimum structure optimized from a force model, showing individual enantiomers in a 6:4 ratio. (Reprinted with permission from Ref. [7]. Copyright 1999, American Physical Society.)

regated chains, 1-nitronaphthalene is able to form chiral decamers [7]. Figure 1.4 shows a cluster of ten 1-nitronaphthalene molecules [8]. The adsorption process on Au {1 1 1} imposes chirality on the molecule and the clusters can be seen to have a pinwheel, chiral conformation, although within the cluster not all the individual molecules have the same handedness. Each cluster contains six molecules of one enantiomer and four of the other. The overall surface is expected to be racemic as regard to both molecules and clusters.

A particularly elegant example of cluster formation involving chiral recognition and retention of chirality through an increasingly complex hierarchical series of clusters is that of rubrene on Au{1 1 1} [9] illustrated in Figure 1.5

The above discussion refers to the loss of mirror symmetry on adsorption leading to chirality at the level of the individual molecule. It is also common for oblique lattices to be formed following molecular adsorption, hence global chirality, even

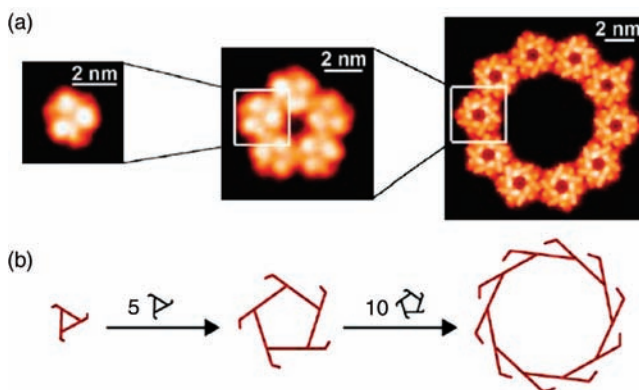


Figure 1.5 (a) Hierarchy of clusters of rubrene on Au{1 1 1}, showing the evolution from trimers to pentamers of trimers and eventually 150 molecules per cluster as a decamer of the pentamers. (b) Illustration of the preservation of chirality through the hierarchy. (Adapted with permission from Ref. [9]).

when the local site retains one or more mirror planes. A specific example of the relationship between local and organizational chirality for a highly symmetric molecule is discussed in some detail in Section 1.2.2.

It is relevant at this point to note that chemistry frequently employs a rather weaker, arguably less precise, definition of chirality than the more “mathematical” definition put forward by Lord Kelvin. A species, which in its most stable conformation has no mirror plane or center of symmetry, is formally chiral but, if there were a low-energy pathway to the enantiomer, for example, by a low-frequency vibrational mode, then, in chemical terminology, this would not normally be considered to be chiral. However, if adsorption of such a species raises the frequency of the vibration substantially, then the energy barrier between the two “enantiomers” may become chemically significant such that the adsorbed molecule is meaningfully described as chiral. An early example of this is the case of the deprotonated glycine species adsorbed on copper surfaces. An isolated glycinate anion, although lacking any mirror plane or center of symmetry, is nevertheless readily converted to its enantiomer principally by a rotation around the C–N bond, with an energy barrier of approximately 35 kJ mol^{-1} , which might readily be overcome at room temperature, such that glycine or glycinate are not generally considered chiral. However, on $\text{Cu}\{1\ 1\ 0\}$, for example, adsorption takes place through both O atoms and the N atom in a tridentate interaction with the copper surface, each atom in an approximately atop site [10, 11]. This inhibits the interconversion of enantiomers, and surface-induced chirality leads to distinct mirror image species on the surface [12]. Nevertheless, unlike the examples discussed above, segregation of enantiomers into clusters, chains, or arrays does not occur. Instead, one molecule of each enantiomer gives rise to a heterochiral (3×2) unit cell and is interrelated by glide lines as shown in Figure 1.6. This proposal based on LEED, STM, and IR data [10] has been confirmed by photoelectron diffraction [11] and by DFT calculations [13]. A suggestion that a second phase consists of homochiral unit cells [12] has not been confirmed by photoelectron diffraction [11, 14] or theory, although the energy difference of this

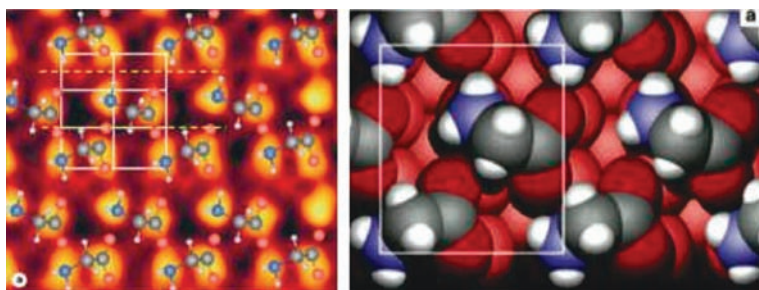


Figure 1.6 The left-hand panel shows a molecular model of the glycinate/ $\text{Cu}\{1\ 1\ 0\}$ structure with both enantiomers present in the heterochiral (3×2) unit cell, superimposed on an STM image of this surface. (Adapted with permission from Ref. [12]. Copyright 2002,

Elsevier.) The right-hand panel shows the confirmation of this structure calculated by DFT, clearly indicating the atop adsorption sites occupied by the N and both O atoms in this system. (Reprinted with permission from Ref. [13]. Copyright 2004, Elsevier.)

phase is calculated to be small (6 kJ mol^{-1}) [13]. It is likely that the different “phases” imaged by STM [12] result from the two rotational domains of the heterochiral structure appearing distinct because of anisotropy in the tip. Interestingly, intrinsically chiral amino acids such as alanine or phenylglycine can adsorb on the Cu{1 1 0} surface also in a (3×2) structure with an apparent glide line indicated by the LEED pattern, although only a single enantiomer is present [15–17].

1.2.2

Lattice Matching

It would seem inherently unlikely that a highly symmetric (D_{6h}) molecule such as coronene, $C_{24}H_{12}$, could give rise to chiral surfaces and indeed diastereoisomeric interactions, particularly when adsorbed on a hexagonal substrate such as graphite or an fcc{1 1 1} face. Nevertheless, we show in this section that lattice matching between an adsorbate overlayer and the substrate can readily give rise to surface chirality, and while this might be unsurprising in systems of lower symmetry, it is still distinctly likely in adsorbate/substrate systems in which both components have inherently high symmetry. To emphasize this aspect, we choose coronene and a related derivative to illustrate how these effects arise from simple interadsorbate interactions and their simple geometric consequences. To simplify matters further, we restrict the adsorption of coronene and its analogues to atop adsorption sites, where symmetry matching with a hexagonal fcc substrate (also locally D_{6h}) would seem to be optimized.

Nondissociative adsorption of coronene on a late transition or coinage metal is likely to be dominated by van der Waals interactions and rather weak π -d interactions, both of which favor a flat-lying and probably atop adsorption geometry again optimizing the symmetry matching. Although relatively weak, these interactions are strong enough to permit stable monolayers to be formed in UHV at room temperature. Interactions between adsorbed coronene molecules are highly isotropic and again dominated by vdW terms. These, therefore, favor hexagonal close packing in an isolated (no substrate) monolayer of planar coronene molecules. Nevertheless, despite all the apparent symmetry matching, it is the subtle energy balance between interadsorbate interactions and those favoring a specific adsorption site, even an atop one, that gives rise to chiral structures and diastereoisomeric effects.

Coronene (Figure 1.7a), considered as a circle, has a vdW diameter of 11.6 \AA , which corresponds to a molecular area of 105.7 \AA^2 and leads, with hexagonal but non-space filling close packing, to a unit cell area of 116.5 \AA^2 . However, coronene on some hexagonal surfaces has an intermolecular separation somewhat less than 11.6 \AA , for example, 11.27 \AA [18] on graphite and 11.18 \AA on MoS_2 [19], suggesting that it is better considered as having a hexagonal, space filling shape with a vdW width of 11.26 \AA . Even this, however, is insufficient to rationalize the intermolecular separations found on other, admittedly nonhexagonal, surfaces such as Cu{1 0 0} [19] and Cu{1 1 0} [20]. In such systems, intermolecular spacings significantly less than 11 \AA can be found. The explanation, while retaining a flat-lying coronene molecule, since there is no evidence to the contrary, lies in recognizing that the 12 H atoms are almost equally

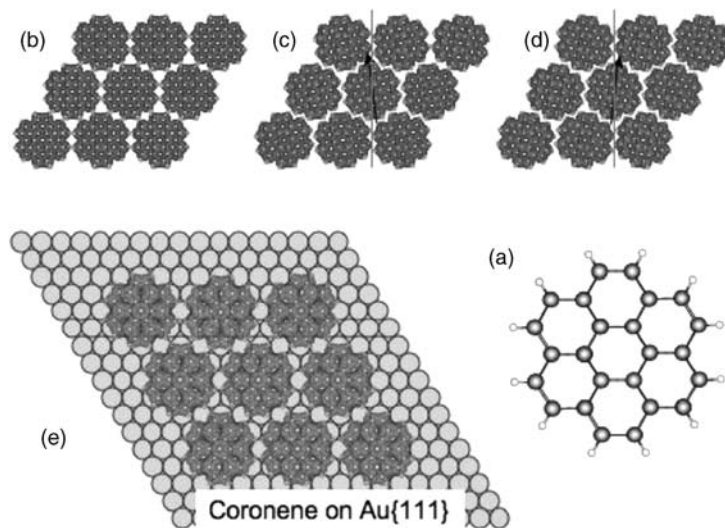


Figure 1.7 (a) Molecular model of coronene; (b) hexagonal close packing at the van der Waals diameter; parts (c) and (d) illustrate the packing advantage, which can be obtained by a concerted rotation, counterclockwise or clockwise, of all molecules to allow

interdigitation of the C–H bonds on adjacent molecules; part (e) illustrates the (4 × 4) model of coronene on Au{111} where the adsorption site dominated separation of molecules is such that interdigitation is unnecessary.

spaced around the periphery of the molecule and confer C_{12} rotational symmetry on the molecule. A concerted rotation of all molecules on the hexagonal lattice by 8.4° about their centers then allows interdigitation of the H atoms on neighboring molecules (Figure 1.7c and d). This permits a 3% reduction of the intermolecular spacing to around 10.9 Å. Herein lies one element of the surface chirality of this molecule.

When the molecules on an isolated hexagonal lattice are rotated in concert away from their initial positions to allow interdigitation and closer packing, the 2D site symmetry is reduced, all mirror planes are lost, and the molecule becomes chiral through the lack of mirror symmetry in the interactions with its neighbors. Rotation to the left or right gives energetically equivalent enantiomers.

There is also a second source of chirality when the adsorbate hexagonal lattice is matched with that of the substrate. For a hexagonal substrate, characterized by unit cell vectors \mathbf{a}_1 and \mathbf{a}_2 aligned along close-packed directions, at 120° to each other and of length a , there are larger hexagonal unit cells defined by unit cell vectors \mathbf{b}_1 and \mathbf{b}_2 , where $\mathbf{b}_1 = m\mathbf{a}_1 + n\mathbf{a}_2$ and $\mathbf{b}_2 = -n\mathbf{a}_1 + (m - n)\mathbf{a}_2$ with m and n integers. These have lengths $b = a\sqrt{(m^2 - mn + n^2)}$ and are rotated $\theta = \tan^{-1}(\sqrt{3}n/(2m - n))$ relative to the substrate unit cell vectors. Many of the smaller ones, based on m and n values up to 6, are familiar overlayers for atomic and molecular adsorbates on fcc{111} substrates, for example, $(\sqrt{3} \times \sqrt{3})R30^\circ$, $(\sqrt{7} \times \sqrt{7})R19.1^\circ$, and so on. For those overlayers where $m = 0$, n , or $2n$, corresponding to rotations of 0° , 60° , and 30° ,

respectively, the structure is achiral since a mirror plane is retained along either the $(1\ 1\ 0)$ or the $(2\ 1\ 1)$ direction. Conversely, if this condition is not met, there is no coincidence of mirror planes between the substrate and overlayer lattices: enantiomeric structures will exist, for example, based on m , n being 3, 1 or 3, 2, that is, $(\sqrt{7} \times \sqrt{7})R19.1^\circ$ and $(\sqrt{7} \times \sqrt{7})R40.9^\circ$, respectively, or perhaps more helpfully described as $(\sqrt{7} \times \sqrt{7})R \pm 19.1^\circ$. Lattice matching of this type giving rise to chiral lattices is common in overlayers on hexagonal substrates, such as the pinwheel structure found for Pd on (1×2) reconstructed $\text{TiO}_2\{1\ 1\ 0\}$ surfaces [21].

In the case of coronene adsorbed on either $\text{Ag}\{1\ 1\ 1\}$ [22] or $\text{Au}\{1\ 1\ 1\}$ [23, 24], an achiral (4×4) structure is observed (Figure 1.7e). This is perhaps unsurprising since this is the hexagonal superlattice that, with a lattice vector of approximately 11.5 Å, is the closest match to the coronene dimensions. Although this lattice is achiral, it demonstrates that the balance between interadsorbate interactions and those favoring a specific adsorption site and hence a commensurate overlayer is important. In contrast, for adsorption of coronene on $\text{Cu}\{1\ 1\ 1\}$, a chiral lattice is predicted based on either $(\sqrt{19} \times \sqrt{19})R \pm 23.4^\circ$ or $(\sqrt{21} \times \sqrt{21})R \pm 10.9^\circ$ lattices. The latter with a unit cell vector of length 11.7 Å might be favored if site preference is strong relative to intermolecular close packing but would not require the concerted rotation of coronene molecules to reduce the intermolecular separation since this is below even the circular diameter of coronene (11.6 Å). Chirality would be limited to that derived solely from the lattice matching and molecules would be free to adopt whatever rotation optimized the energy based on an atop local site geometry. Of course, a twist away from a high-symmetry azimuthal orientation, which might be clockwise or anticlockwise, introduces a second chiral element and hence the need to consider diastereoisomerism. There are four possible choices of lattice/molecular twist that might conveniently be designated $+/+$, $-/-$ for one pair of enantiomers and $+/-$, $-/+$ for the other pair. In principle, a particular sense of rotation could favor a particular lattice orientation such that one pair is energetically more favorable than the other. However, since intermolecular interactions are likely to be weak at this separation, the energy difference is likely to be small. This contrasts with the situation if the former lattice, $(\sqrt{19} \times \sqrt{19})R \pm 23.4^\circ$, were preferred because of the importance of intermolecular interactions. In this case, since the substrate imposed lattice dimension is only 11.14 Å, molecular rotation imposed within the 2D adsorbate lattice is required, with C–H interdigitation to achieve this reduced separation as shown in Figure 1.8. The second element of chirality is again a molecular rotation but one that has its origin in the intermolecular interactions rather than molecule–substrate site interactions. The energy preference between the two diastereoisomer pairs is now dictated by which pair leads to the more favorable orientation of the molecule on the atop adsorption site. Notable, perhaps, is that for one diastereoisomer pair the azimuthal orientation of the molecule with respect to the substrate is such that a local high symmetry is recovered because the lattice rotation of 23° , combined with the optimum interdigitation rotation of 8° , realigns the mirror planes of the molecule very closely ($<2^\circ$) with those of the substrate. To our knowledge, coronene adsorption on $\text{Cu}\{1\ 1\ 1\}$ has not been studied, but clearly this system would provide an interesting model for investigating the subtle energy